International Journal of Advanced Research in

Electrical and Electronics Engineering

Volume: 3 Issue: 1 26-Jun-2014,ISSN_NO: 2321-4775

Advanced electric vehicle system Using Choppers

Kartheeswaran[1], kirubasankar[2],karthikeyaen[3]
1Department of Electrical and Electroni Engineering, Velammal Institute of Technology, Chennai (TN), INDIA.
2Department of Electronics and communication Engineering Department, Velammal Institute of Technology Chennai (TN), INDIA
3Department of Electronics and communication Engineering, Velammal Institute of Technology, Chennai (TN), INDIA.

ABSTRACT--*Batteries are the primary energy-storage devices in ground vehicles. Now days battery fed electric drives are commonly being used for electric vehicles applications, due to various advantages, such as: nearly zero emission, guaranteed load leveling, good transient operation and energy recovery during braking operation. To fulfill these requirements converters with bidirectional power flow capabilities are required to connect the accumulator (battery) to the dc link of the motor drive system. Battery fed electric vehicles (BFEVs) is required to function in three different modes namely: acceleration mode, normal (steady-state) mode and braking (regenerative) mode. During acceleration and normal modes the power flow is from battery to motor whereas during braking or regenerative mode the kinetic energy of the motor is converted into electrical energy and fed back to battery. The DC-DC converter is required to perform mainly two functions: first to match the battery voltage to the motor rated voltage and second to control the power flow under steady-state and transient conditions, so that the drive performance is as per the requirement. In the present work closed loop operation of bi-directional dc-dc converter feeding a dc motor and its energy recovery due to regenerative braking has been demonstrated. The characteristics of battery operated electric vehicle under different drive condition are also presented. The effectiveness of the system is verified through the simulations using Simulink/ MATLAB 7.6.0 (R2008a) package.*

Keywords: Bi-directional dc-dc converter, separately excited dc motor, Battery.

This paper deals with the use of a Bi-directional dc-dc converter for a battery fed electric vehicle drive system. A closed loop speed control technique of the proposed battery fed electric vehicle is designed and implemented using PI controller. The overall drive system reduces the system complexity, cost and size of a purely electric based vehicular system.

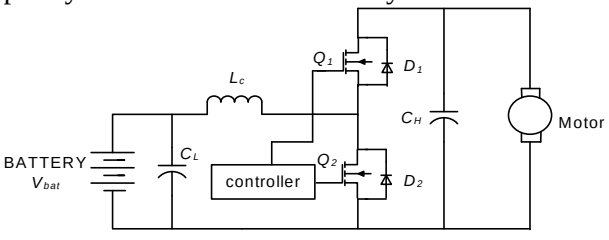

Above figure shows the proposed Bi-directional dc-dc converter fed DC motor drive. In this topology, boost converter operation is achieved by modulating Q_2 with the anti-parallel diode D_1 serving as the boost-mode diode. With the direction of power flow reversed, the topology functions as a buck converter through

Volume: 3 Issue: 1 26-Jun-2014,ISSN_NO: 2321-4775

the modulation of Q_1 , with the anti-parallel diode D_2 serving as the buck-mode diode.It should be noted that the two modes have opposite inductor current directions. A new control model is developed using PI controller to achieve both motoring and regenerative braking of the motor. A Lithium-ion battery model has been used in this model to verify the motor performance in both motoring and regenerative mode. This controller shows satisfactory result in different driving speed commands.

For the dc–dc converter, the only important part of the inverter–machine subsystem is the zero-sequence impedance and the zero-sequence voltage vz . Thus, the integrated dc–dc converter can be modeled. The time-dependent voltage source vzrepre- sents the zero-sequence voltage and vs4 describes the voltage across ss4 . These two voltage sources are con- nected to an LR circuit, modeling the machine's zero-sequence impedance. Voltage vt represents the transformer voltage. It has to be mentioned that vz, can only be measured if no zero-sequence current flows; otherwise, it is a theoretical quantity since there is a voltage drop vlr across L0 and R0. The voltage measured between the star point and the negative bus is equal to vz −vlr. This system is similar to a full-bridge rectifier system, but as the voltage vz applied to the system is neither average free (related to the switching frequency) nor free from even harmonics, a conventional modulation scheme cannot be adopted. In the actual implementation, an active rectifier is used to guarantee that the voltage-time product across the transformer remains below a predetermined level. The described dc–dc con- verter is similar to a dual active bridge. A unidirectional implementation with a diode rectifier would be an-Converter waveforms: zero-sequence voltage vz , voltage vs4 across s4, voltage vt1 across st1, voltage vt2 across st2, and transformer voltage vt.

other possibility, but in order to limit the voltage-time product across the transformer, a special control approach has to be implemented.

2. Circuit Description

*2.1 Converter operation:*The bidirectional dc-dc converter shown in Figure1 is operated in continuous conduction mode for forward motoring and regenerative braking of the dc motor. The MOSFETs Q_1 and Q_2 are switched in such a way that the converter operates in steady state with four sub intervals namely interval *1*(t_0-t_1), interval *2*(t_1-t_2), interval *3*(t_2-t_3) and interval *4*(t_3t_4). It should be noted that the low voltage battery side voltage is taken as V_1 and high voltage load side is taken as V_2. The gate drives of switches $Q_1$and $Q_2$are shown in Figure 3. The circuit operations in steady state for different intervals are elaborated

Volume: 3 Issue: 1 26-Jun-2014,ISSN_NO: 2321-4775

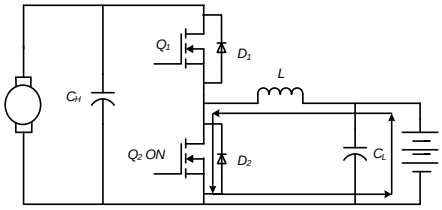

(a)Interval (t0-t1).

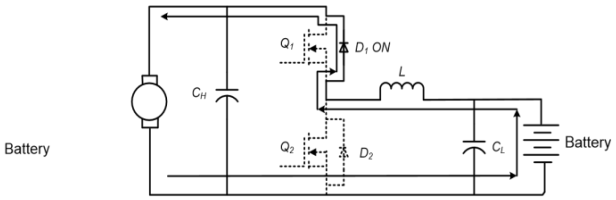

(cInterval(t_2-t_3).

(d) Interval (t_3-t_4).

Battery

1 2

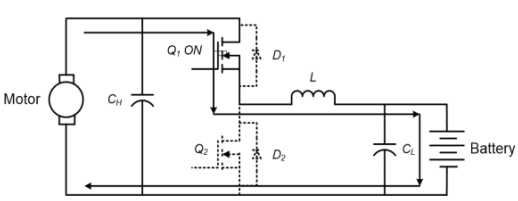

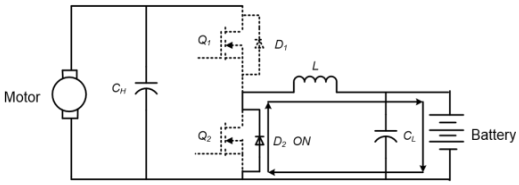

Figure 2. Converter operating modes.

2.1.1 Interval 1(t_0-t_1): At time t_0,the lower switch Q_2 is turned ON and the upper switch Q_1 is turned OFF with diode D_1, D_2 reverse biased as shown in Figure 2(a). During this time interval the converter operates in boost mode and the inductor is charged and current through the inductor increases.

$$L_c + \frac{di_L}{dt} = V^2 \quad (1)$$

2.1.2 Interval 2(t_1-t_2): During this interval both switches Q_1 and Q_2 is turned OFF. The body diode D_1 of upper switch Q_1 starts conducting as shown in Figure 2(b). The converter output voltage is applied across the motor. As this converter operates in boost mode is capable of increasing the battery voltage to run the motor in forward direction.

$$\frac{\boldsymbol{di_a}}{\boldsymbol{dt}} = \frac{V_1}{L_a} - \frac{E_b}{L_a} - \frac{r_a}{L_a}\mathbf{i_a} \quad (\mathbf{2})$$

$$\frac{\mathrm{d}V_1}{\mathrm{dt}} = \frac{i_a}{C_h} \quad (3)$$

$$\frac{\mathrm{d}V_2}{\mathrm{dt}} = \frac{V_b}{R_b.C_1} - \frac{V_2}{R_b.C_1} - \frac{i_L}{C_1} \quad (4)$$

Interval 3(t_2-t_3): At time t_3, the upper switch Q_1 is turned ON and the lower switch Q_2 is turned OFF with diode D_1, D_2 reverse biased as shown in Figure 2(c). During this time interval the converter operates in buck mode.

(b) Interval (t1 –t2)

$$\frac{di_L}{dt} = \frac{-V_1}{L_c} + \frac{V_2}{L_c} - \frac{i_L}{C_1} \quad (5)$$

$$\frac{dV_2}{dt} = \frac{V_b}{R_b.C_1} - \frac{V_2}{R_b.C_1} - \frac{i_L}{C_1} \quad (6)$$

2.1.3 *Interval 4(t_3-t_4):* During this interval both switches Q_1 and $Q_2$is turned OFF. The body diode $D_2$of lower switch Q_2 starts conducting as shown in Figure 2(d).

$$\frac{dV_1}{dt} = \frac{i_L}{C_h} + \frac{i_a}{C_h} \quad (7)$$

$$\frac{di_a}{dt} = \frac{V_1}{L_a} - \frac{E_b}{L_a} - \frac{r_a}{L_a} i_a \quad (8)$$

The state space average model is shown in (9) and (10).

$$0 = \mathbf{A}.\begin{vmatrix} i_L \\ i_a \\ V_1 \\ V_2 \end{vmatrix} + \mathbf{B}.\begin{vmatrix} E_b \\ V_b \end{vmatrix} \quad (9)$$

Volume: 3 Issue: 1 26-Jun-2014,ISSN_NO: 2321-4775

$$\mathbf{A} = \begin{vmatrix} 0 & 0 & \frac{-(1-D)}{L_c} & \frac{1}{L_c} \\ 0 & \frac{-R_a}{L_a} & \frac{1}{L_a} & 0 \\ \frac{(1-D)}{C_h} & \frac{-1}{C_h} & 0 & 0 \\ \frac{-1}{C_1} & 0 & & \end{vmatrix}$$

$$\mathrm{B} = \begin{vmatrix} 0 & 0 \\ \frac{-1}{L_a} & 0 \\ 0 & \frac{1}{R_b.C_l} \end{vmatrix} \qquad (10)$$

Figure 3 shows the gate pulses of the upper and lower switches of the Bi-directional converter and is switched alternatively without any dead time in between. The control signals are obtained by comparing the modulating signal $V_{triangular}$ with the carrier signal $V_{control.}$

2.2 Converter design: The bi-directional converter is designed based on the input supply voltage and output voltage requirement to drive the electric vehicle at desired speed. The converter power topology is based on a half bridge circuit to control the dc motor. At a given input battery voltage and reference speed command the inductor current has a nearly constant peak to peak swing. The inductor is designed with a specified current ripple of 15A and 20 KHz switching frequency. *D2 Q2 D1 Q1 D2*

Equations (11)-(13) are used to design the converter. t0

t1 t2 t3 t4

Figure 3. Complementary Gate Pulses

$$\Delta \mathrm{I} = \frac{1}{2}.\frac{V_2 - V_1}{L_c}.\frac{V_1}{V_2}.T_s$$

$$I_a = \frac{P}{V_2}$$

$$I_{rms} = \sqrt{I_{Load}^2 + \frac{\Delta I^2}{3}} \qquad (13)$$

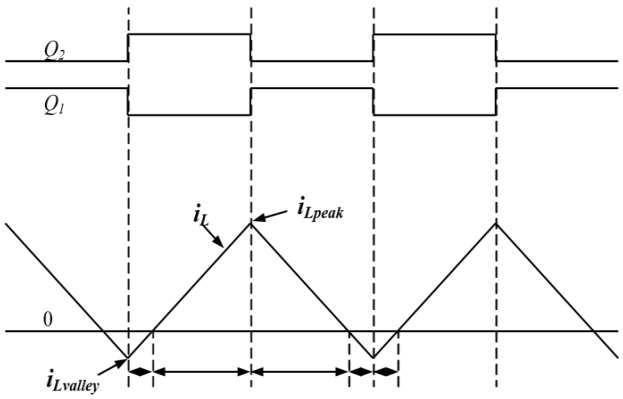

2.3 DC motor modeling: The modeling of the DC motor has been carried out with torque and rotor angle

consideration. The steady state motor torque T is related to armature current I and a torque constant K.

$T_m = KI_a$ (14)

The back emfE_b, is related to angular velocity by

$$E_b = K_{\omega_m} = K\frac{d\theta}{dt} \quad (15)$$

$$j\frac{d^2\theta}{dt^2} + B\frac{d\theta}{dt} = KI_a \quad (16)$$

$$L\frac{dI_a}{dt} + RI_a = V - K\frac{d\theta}{dt} \quad (17)$$

Transfer function using Laplace transformation, equations (16) and (17) can be written as

$Js^2\theta(s) + bs(\theta) = kI_a(s)$ (18)

$$LsI(s) + RI(s) = V(s) - K_s\theta(s)$$

(19)

where, *s* denotes the Laplace operator.

From equation (19), the current can be expressed as

$$I(s) = \frac{V(s) - K\theta(s)}{R + L_s}\pi r^2 \quad (20)$$

$$Js^2\theta = bs\theta(s)\frac{K(V(s) - K_s\theta(s)}{R + L_s} \quad (21)$$

From equation (21), the transfer function from the input voltage V(s) to the output angle θ can be written as

$$G_a(s) = \frac{\theta(s)}{V(s)} = \frac{K}{\{s[(R + Ls)(Js + b) + K^2]\}} \quad (22)$$

The transfer function from the input voltage V(s) to the angular velocity ω(s) is,

Volume: 3 Issue: 1 26-Jun-2014,ISSN_NO: 2321-4775

$$G_v(s) = \frac{\omega(s)}{V(s)} = \frac{K}{[(R + Ls)(Js + b) + K^2]} \quad (23)$$

3. Control Strategy

The control circuit of the bidirectional converter is shown in Figure 4.To control the speed of the dc drive; one possible control option is to control the output voltage of the bidirectional converter. To control the output voltage of the bidirectional converter for driving the vehicle at desired speed and to provide fast response without oscillations to rapid speed changes a PI controller is used and it shows satisfactory result. In this control technique the motor speed ω_m is sensed and compared with a reference speed ω_{ref}. The error signal is processed through the PI controller. The signal thus obtained is compared with a high frequency saw tooth signal equal to switching frequency to generate pulse width modulated (PWM) control signals. High frequency

The block diagram of feedback speed control system for DC motor drive is shown in Figure 5; the control objective is to make the motor speed follow the reference input speed change by designing an appropriate controller. The proportional-integral(PI) controller is used to reduce or eliminate the steady state error between the measured motor speed (ω_{motor}) and the reference speed (ω_{ref}) to be tracked. The transfer function of PI controller is given by

$$G_c(s) = K_p + \frac{K_i}{s} \quad (24)$$

Where, $K_P$and K_i are the proportional and integral gains. The value of $K_P$and $K_i$are obtained by using Zeigler Nichols tuning method. Simulink model of the overall system is shown in figure 5.

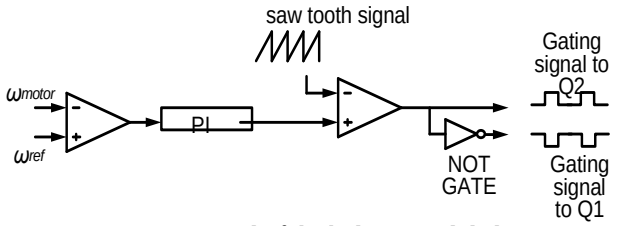

Figure 4. Control of the bidirectional dedc converter.

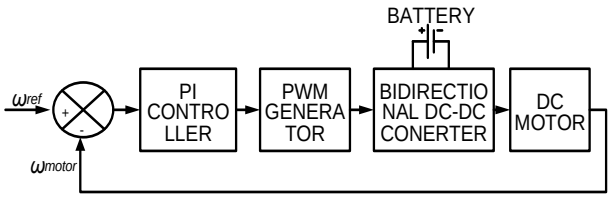

Figure 5. Closed loop operation of the drive.

Volume: 3 Issue: 1 26-Jun-2014,ISSN_NO: 2321-4775

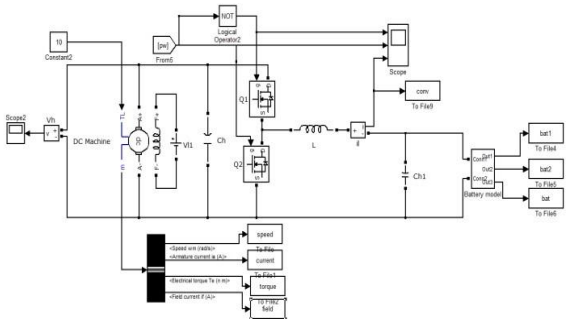

Figure 5. Simulink Model of the Drive system.

4. Battery Requirement for Automotive Application.

Mainly Nickel-Metal hydride (NiMH) and Lithium-ion batteries are used in vehicular application due to their characteristics in terms of high energy density, compact size and reliability. The battery is being recharged by the regenerative capabilities of the electric motors which are providing resistance during braking helping to slow down the vehicle.

The lithium-ion battery has been proven to have excellent performance in portable electronics and medical devices .The lithiumion battery has high energy density, has good high temperature performance, and is recyclable. The promising aspects of the Li-ion batteries include low memory effect, high specific power of 300 W/kg, high specific energy of 100 Wh/kg, and long battery life of 1000 cycles. These excellent characteristics give the lithium-ion battery a high possibility of replacing NiMH as next-generation batteries for vehicles. Equation (25) is used to estimate the state of charge (SOC) of the battery.

$$V_{soc}(t) = V_{soc}(0) - \frac{1}{C_{CAP}} \int_0^{\tau} i(t) d\tau \qquad (25)$$

5. Simulation R

Performance of the dc motor drive with the above battery model and bidirectional converter is simulated under different speed command. The simulations are carried out using MATLAB/SIMULINK. The inductor parasitic resistance and MOSFET turn-on resistance are not considered in this case. For the test condition of the proposed drive topology the following values of the different components of the converter are considered.A separately excited DC motor model is used as load to the bidirectional dc-dc converter. The motor rated at 5 hp, 240 V, and 1750 rpm.

Principal parameters of the bidirectional converter are: *L = 1600 µH, C_H=470 µF, C_L = 470 µF, f_{SW}=20 kHzBattery voltage=48 V. Battery capacity=16 Ah, SOC=88%.*

A total of two cases of the drive system are studied:1) steady state operation : the reference motor speed is 120rad/sec with a constant torque demand of 10Nm, 2) transient state operation: case (I) when the speed changes from 60 rad/sec to 120 rad/sec with a constant torque demand of 10 Nm at time t=5 secs and case (II) regenerative braking mode: the speed changes from 120 rad/sec to 0 rad/sec. Torque changes from +10

Volume: 3 Issue: 1 26-Jun-2014,ISSN_NO: 2321-4775

Nm to -10 Nm at a step time of 5 secs. The simulation is carried out for (a) motor speed, (b) torque, (c) motor current, (d) battery state of charge (SOC), (e) battery voltage, (f) battery current, (g) battery power and motor power and (h) battery energy and motor energy characteristic during regenerative braking mode.

Case I. Steady State Results.

Figure 6(a) shows the simulation result of the drive system at a reference speed of 120rad/sec for a total simulation time of 10 sec. Motor speed reaches at its steady state speed of 120 rad/sec at time less than 0.5 sec. Figure 6(b) (c) shows the motor torque and current of the drive respectively. The battery SOC was initially set at 88%, Figure 6(d) shows the SOC of the battery, when the drive was running for 10 sec at a speed of 120rad/sec. Figure 6(e) and (f) show the battery voltage and current under this condition. Figure 6(g) shows the comparison between the battery power and motor power.

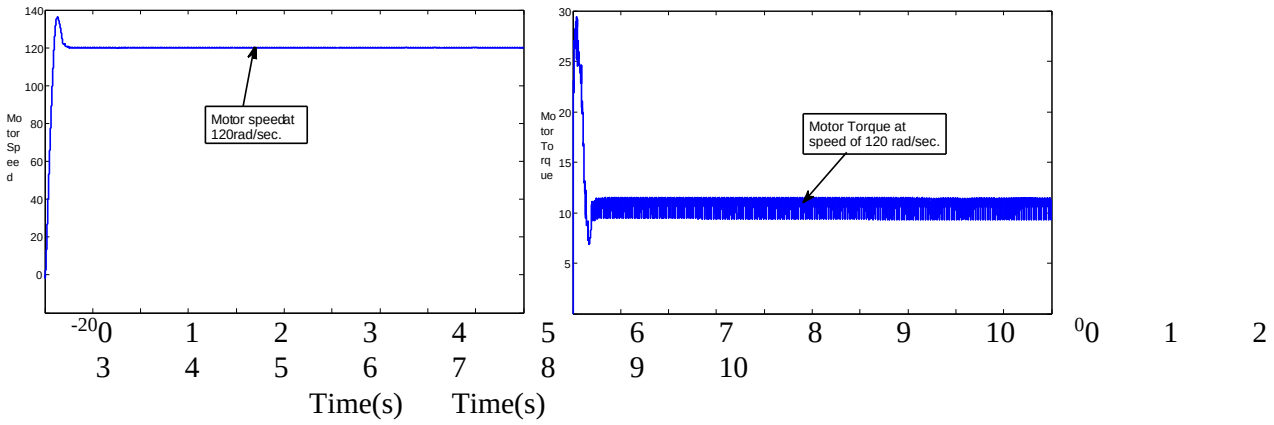

Figure 6(a). Motor speed

Figure 6(b). Motor Torque

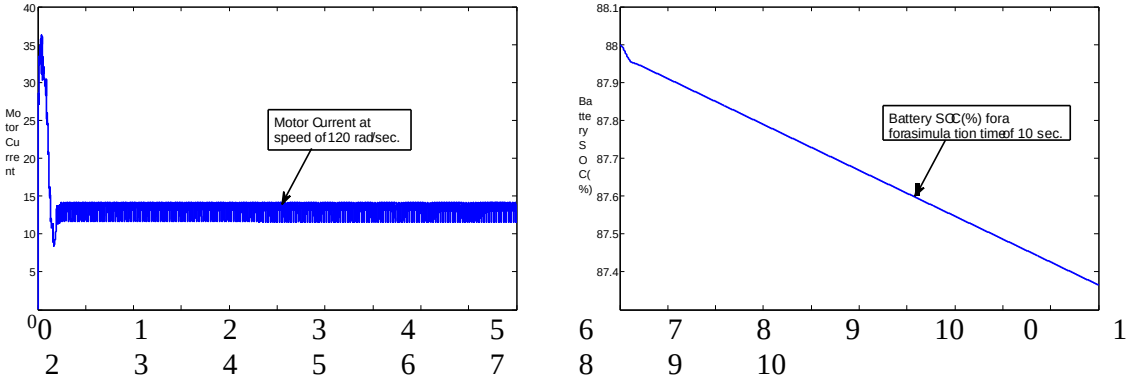

Figure 6(c). Motor current

Figure 6(d). Battery State of charge

Volume: 3 Issue: 1 26-Jun-2014,ISSN_NO: 2321-4775

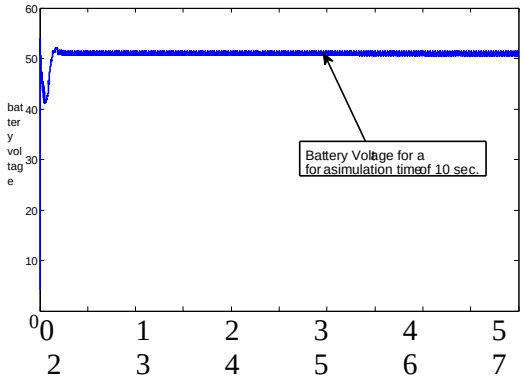

Figure 6(e). Battery voltage.

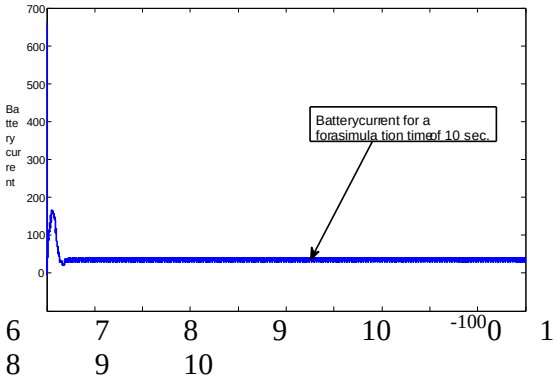

Figure 6(f). Battery current.

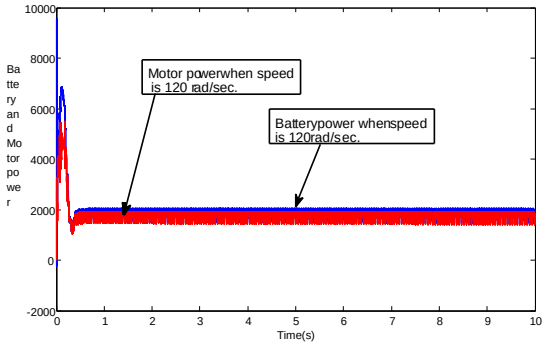

Figure 6(g). Motor and battery power.

Figure 6. Simulation result under steady state condition (motoring mode), speed reference 120 rad/sec, simulation time of 10sec, at constant torque of 10Nm.

Case II. Transient State Results.

During transient, simulations are performed when the motor speed is changed from 60rad/sec to 120rad/sec. Figure 7(a) shows the speed curve under this condition for time of 5 sec. Figure 7(b) shows that the momentarily increase in torque when there is a sudden change in speed requirement. Figure 7(c) indicates the current which is same as the torque characteristic. When the speed increases, the motor draws more power from the source as shown in figure 7(d), the battery SOC. Figure 7(e) (f) shows the battery voltage and current under this condition. Figure 7(g) indicates the power management curve of motor and battery under the same operating condition. Figure 7(h) shows the battery and motor energy during the transient operation. These results show the satisfactory performance of drive under the step-up transients.

Simulations are also performed for the braking operation when the speed is changed from 120 rad/sec to 100 rad/sec while the motor torque and current has reverse characteristic as shown in Figure 8(a), (b) and Figure 8(c) respectively. Figure 8(d) shows the battery SOC during regenerative braking mode. Figure 8(e) and (f) shows the battery voltage and current respectively. Figure 8(g) shows the characteristics of motor power and battery power under the same drive condition. Figure 8(h) shows the battery energy characteristic in regenerative braking mode. The energy recovered by the battery in this mode is 3000J. The observation on

Volume: 3 Issue: 1 26-Jun-2014,ISSN_NO: 2321-4775

steady state and transient state are shown in Table I. These results show the satisfactory performance of drive under the step-down transients.

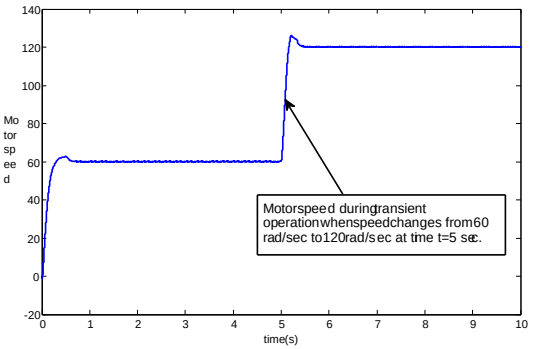

Figure 7(a). Speed.

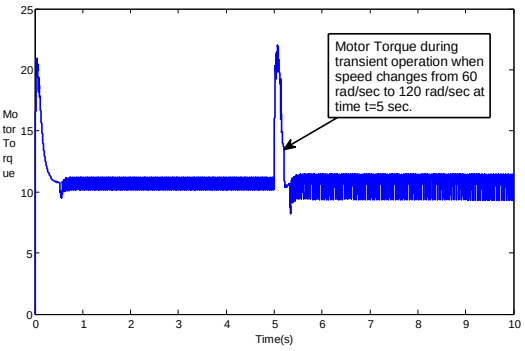

Figure 7(b). Torque

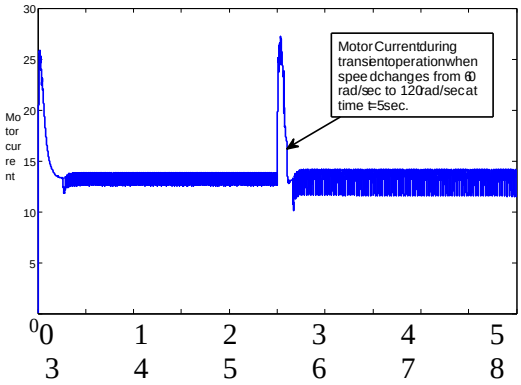

Figure 7(c). Motor current

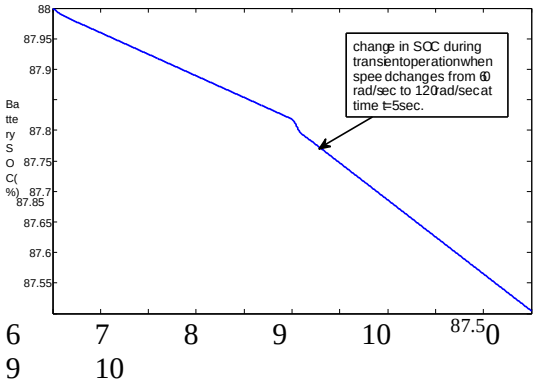

Figure 7(d). Battery SOC.

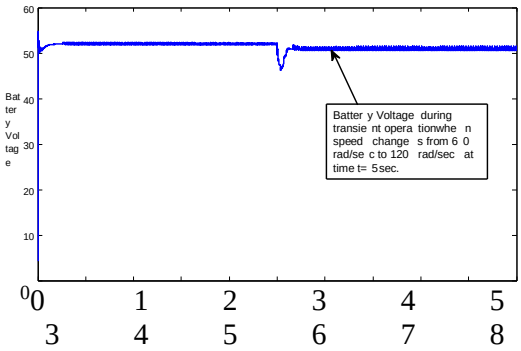

Figure 7(e). Battery voltage.

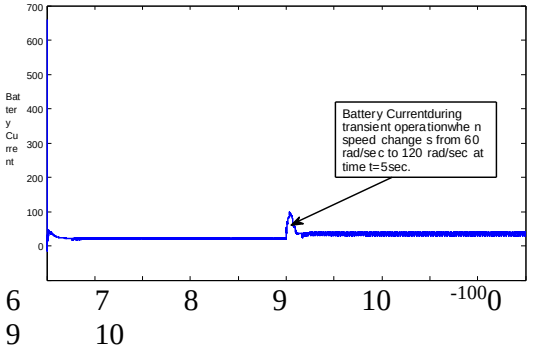

Figure 7(f). Battery current.

International Journal of Advanced Research in

Electrical and Electronics Engineering

Volume: 3 Issue: 1 26-Jun-2014,ISSN_NO: 2321-4775

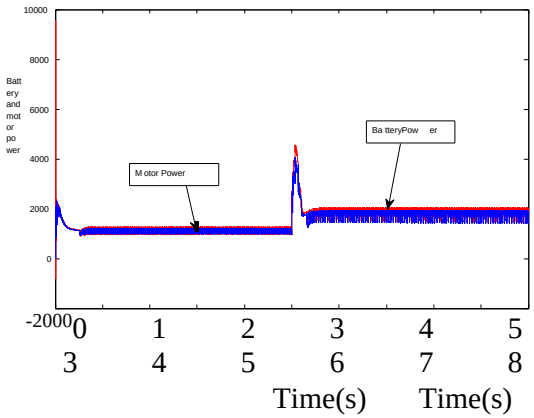

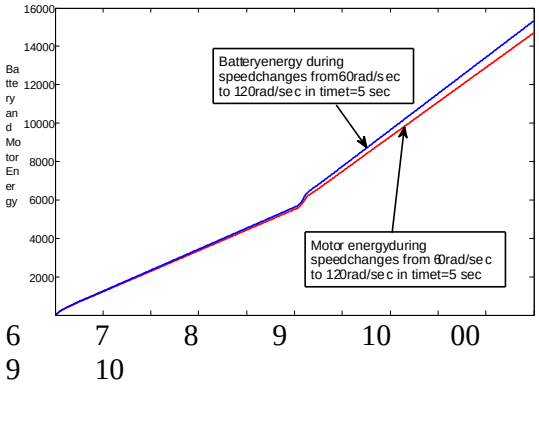

Figure 7(g). Motor and battery power. **Figure 7(h).** Battery and Motor energy.

Figure 7. Simulation result under motoring mode, speed reference 60 to 120 rad/sec with time step of 5sec.

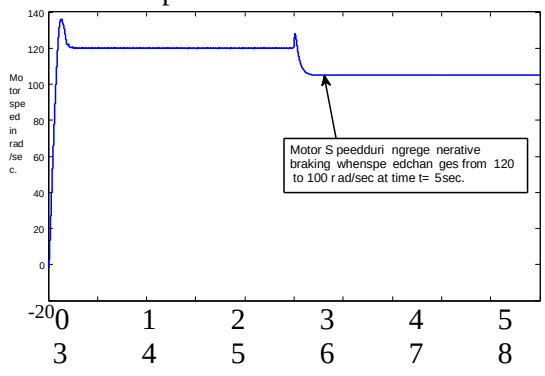

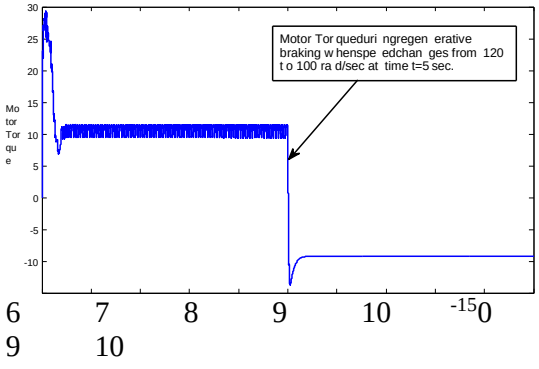

Figure 8(a). Motor speed. **Figure 8(b).** Motor torque.

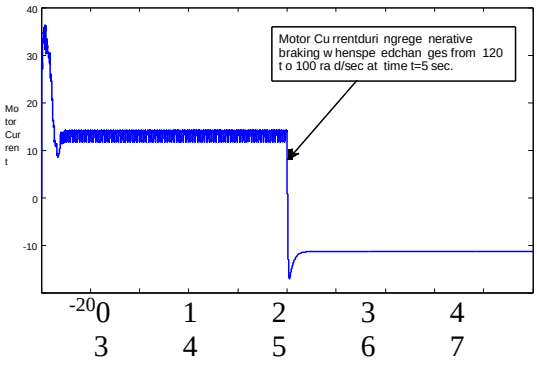

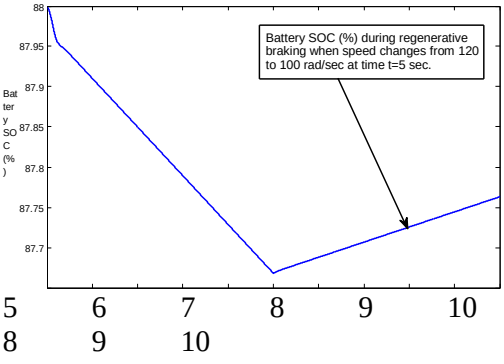

Figure 8(c). Motor current **Figure 8(d).** Battery State of charge.

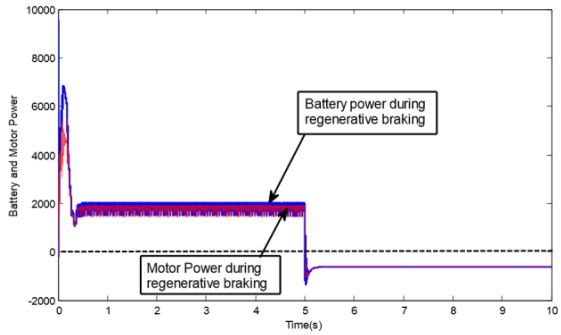

Figure 8(e). Motor and Battery power energy

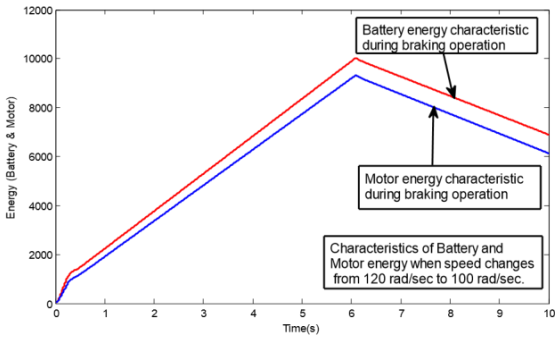

Figure 8(f). Battery and motor

Figure8. Simulation result under regenerative braking mode, speed reference 120 to 0 rad/sec with time step of 5sec when torque changes from 10Nm to -10Nm.

Table1. Observations

Figure no.	Observations	Remarks
Figure 6	Steady state operation, Battery power=2000w, Motor power=1920w	Battery SOC reduced from 88% to 87.3%.
Figure 7	Transient operation, Speed changes from 60rad/sec to 120 rad/sec. Battery power changes from 1600 to 2000w, Motor power changes from 1520 to 1920w.	Battery SOC reduced from 88% to 87.5%.
Figure 8	Transient operation (regenerative braking mode) Ia is positive (0<t<5sec), Ia is negative(5sec<t<10sec)	Energy recovered due to due to braking operation=3000J

6. Conclusions

In this work we demonstrate the performance of a battery operated electric vehicle system and it shows satisfactory performance at different driving condition. The proposed control technique with PI controller find suitable for this electric drive. The performance of the BFEV is verified under forward motoring mode, regenerative mode and when there is step change is speed command. The overall cost and volume of the battery operated electric vehicle is less with the least number of components used in the system.

References

Jain P.K., Kang W., Soin H., Xi Y., 2002 Analysis and design consideration of a load and line independent Zero voltage switching Full bridge DC/DC Converter topology, *IEEE Transaction on Power Electronics*, Vol.17, No.5, September. pp 649-657.

Yu W., Lai J.-S., 2008. Ultra High Efficiency Bidirectional DC-DC Converter With multi frequency pulse width modulation APEC 2008,pp 1079-1084.

Zhang J., Lai J.-S., Kim R.-Y., Wensong Yu, 2007. High power density design of a soft-switching high-power bidirectional dc-dc converter, IEEE Transactions on power electronics, Vol.22, No.4, pp 1145-1153, July.

Zhang Y., Sen P.C., 2003. A new soft switching technique for buck, boost, and buck-boost converters, *IEEE transactions on Industry Applications*, Vol. 39. No.6, November/December, pp. 1775-1782.

Zhang J., Lai J.-S., Yu W., 2008. bidirectional dc-dc converter modeling and unified controller with digital implementation, *Applied Power Electronics Conference and Exposition*, APEC 2008, pp.1747-1753, Feb.

S. Williamson, M. Lukic, and A. Emadi, "Comprehensive drive train efficiencyanalysisofhybridelectricandfuel cell vehicles based on motor- controller efficiency modeling," IEEE Trans. Power Electron., vol. 21, no. 3, pp. 730–740, May 2006.

A. Emadi, S. Williamson, and A. Khaligh, "Power electronics intensive solutions for advanced electric, hybrid electric, and fuel cell vehicular power systems," IEEE Trans. Power Electron., vol. 21, no. 3, pp. 567–577, May 2006.

A. Emadi, M. Ehsani, and J. Miller, "Advanced silicon rich automotive electrical power systems," in Proc. 18th Digit. Avionics Syst. Conf., St Louis, MO, Oct. 24–29, 1999, vol. 2, pp. 8.B.1-1–8.B.1-8.

J. Wang, F. Peng, J. Anderson, A. Joseph, and R. Buffenbarger, "Low cost fuel cell converter system for residential power generation," IEEE Trans. Power Electron., vol. 19, no. 5, pp. 1315–1322, Sep. 2004.

K. Moriya, H. Nakai, Y. Inaguma, H. Ohtani, and S. Sasaki, "A novel multi-functional converter system equipped with input voltage regulation and current ripple suppression," in Conf. Rec. 2005 Ind. Appl. Conf. 40th IAS Annu. Meeting, Oct. 2–6, vol. 3, pp. 1636–1642.

Biographical notes

Kartheeswaranis currently pursuing UG degree in Electrical and Electronics Engineering at Velammal Institute Of Technology, Chennai, India. His interests are Power Electronics, dc-dc converters, electric drives.

kirubasankarcurrently pursuing UG degree in Electronics and communication Engineering at Velammal Institute Of Technology, Chennai, India. His interests are Power Electronics, dc-dc converters, electric drives

Karthikeyan.M.E., professor UG degree in Electronics and Communication Engineering at Velammal Institute Of Technology, Chennai, India. His interests are Power Electronics, dc-dc converters, electric drives.

.